

Critical Slowing Down of Triangular Lattice Spin-3/2 Heisenberg Antiferromagnet Li_7RuO_6 via ^7Li NMR

YUTAKA ITOH^{1*}, CHISHIRO MICHIOKA¹, KAZUYOSHI YOSHIMURA¹,
KANAKO NAKAJIMA², and HIROHIKO SATO²

¹*Department of Chemistry, Graduate School of Science, Kyoto University, Kyoto 606-8502*

²*Department of Physics, Chuo University, 1-13-27 Kasuga, Bunkyo-ku, Tokyo 112-8551*

We report ^7Li NMR studies of single crystals of triangular-lattice Heisenberg antiferromagnet Li_7RuO_6 . Slow critical divergence with a wide critical region of $|T/T_N - 1| \leq 7$ was observed in ^7Li nuclear spin-lattice relaxation rate. The slowing down of staggered spin fluctuations was analyzed in a renormalized classical region of a two-dimensional triangular-lattice non-linear sigma model. A spin stiffness constant was found to reduce to about 20 % from the value in a spin-wave approximation. The effect of spin frustration, e.g., Z_2 vortex excitations on the critical phenomena is suggested.

KEYWORDS: Li_7RuO_6 , triangular lattice, spin frustration, NMR, renormalized classical region

Spin frustration effect of a triangular lattice Heisenberg antiferromagnet has been one of the central issues in physics and chemistry of magnetic insulators. The ground state is classically a long range ordering state with the 120° spin structure, but the quantum mechanical ground state might be a gapped or gapless quantum spin liquid.¹⁻³ Elementary excitations of Z_2 vortices, topologically stable point defects, are inherent even in classical triangular spin systems.⁴⁻⁷ At finite temperatures, topological phase transition between the paramagnetic states is theoretically predicted from numerical simulations.

Finite-temperature magnetic long range ordering of quasi low dimensional antiferromagnets may be ascribed to a three dimensional interaction and the anisotropy. The low dimensional characteristics are (i) the suppressed magnetic ordering temperature $T_N < T_N^{\text{MF}}$ in the mean field approximation, (ii) the suppressed Curie-Weiss law, i.e., the maximum of uniform spin susceptibility at T_{max} due to short range ordering, and (iii) a wide critical region in two dimensions.³

Two dimensional square lattice Heisenberg antiferromagnet has been intensively studied through the studies of high- T_c cuprates.^{2,3} Our understanding a short range ordering has made rapid progress. In the renormalized classical region, an antiferromagnetic correlation length and a staggered spin susceptibility diverge exponentially toward $T_N = 0$ K,^{8,9} which were observed in La_2CuO_4 .^{10,11} Such a wide critical region toward $T_N = 0$ K is the notable feature of two dimensional square lattice Heisenberg antiferromagnets. Non-linear sigma model and field theoretical treatments turned out to be the relevant model and to give us powerful methods to describe the low energy excitations. They were also applied to the non-collinear frustrated magnetic systems like the triangular lattice.¹²⁻¹⁷ To our knowledge, however, the theoretical critical behavior has not been widely tested to the actual critical phenomena of triangular spin systems.

A delafossite-type Li_7RuO_6 has been at first reported as hexagonal " $\text{Li}_{8-\delta}\text{RuO}_6$ ".¹⁸ However, a detailed analysis on powder¹⁹ and on single crystal²⁰ revealed that the actual composition is " Li_7RuO_6 " and the structure is slightly distorted from an ideal hexagonal lattice. Li_7RuO_6 is triclinic and has the superlattice structure of the Li deficiency in the double Li layers.²⁰ Figures 1(a) and 1(b) show the crystal structure and the triangular lattice, respectively. Single Li_2RuO_6 layer and double Li layers are stacked with each other. The Li_2RuO_6 layer consists of a triangular lattice of RuO_6 octahedrons and a Li honeycomb lattice. The Li ions occupy 12 sites in the RuO_6 layer and 30 sites in the Li deficient layers in unit cell, which are crystallographically inequivalent. For

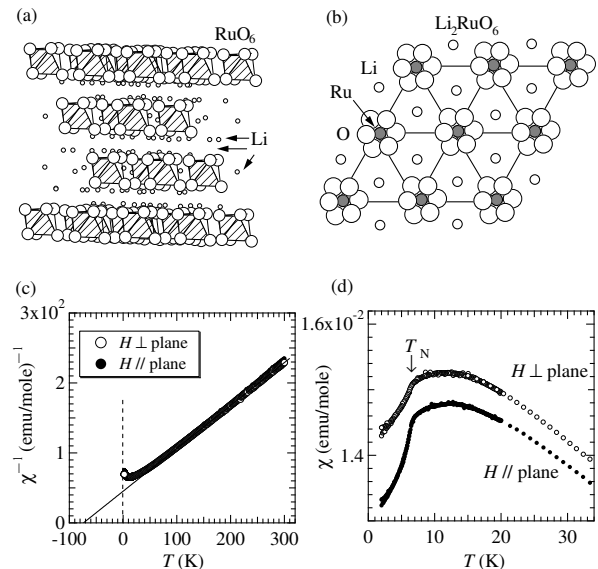


Fig. 1. (a) Schematics of crystal structure of Li_7RuO_6 and (b) the top view of a triangular lattice Ru plane. (c) Inverse magnetic susceptibility χ^{-1} and (d) the magnetic susceptibility χ of a single crystal Li_7RuO_6 . The solid lines are the best fits by an inverse Curie-Weiss law. The arrow indicates $T_N \approx 6.5$ K.

*E-mail: itoh@kuchem.kyoto-u.ac.jp

a hexagonal model of Li_3RuO_6 , the staggered magnetic field from Ru would be cancelled out at the Ru-plane Li site. However, for the actual Li_7RuO_6 , since the Li ions occupy non-ideal positions deviated from the center of the Ru triangle, then the 120° staggered spin fluctuations can be probed through the Li NMR. Li_7RuO_6 is a deformed triangular lattice system. The detail of the crystal growth and the structure analysis will be published in a separated paper.²⁰

Uniform magnetic susceptibility χ_α ($\alpha = \parallel$ and \perp denote $H \parallel$ plane and $H \perp$ plane) shows a slightly anisotropic Curie-Weiss behavior $\chi = C/(T - \Theta)$ with $C = 1.89$ emu/mol·Ru and $\Theta = -73$ K at high temperatures. Figures 1(c) and 1(d) show the inverse magnetic susceptibility χ^{-1} up to 300 K and the magnetic susceptibility χ on an enlarged scale for a single crystal, respectively. Upon cooling, χ_α makes a maximum at about 12.5 K and drops sharply at the Neel temperature $T_N \approx 6.5$ K.^{19,20} The broad maximum behavior indicates a low dimensional magnet. The Curie constant C is close to the value for $S = 3/2$ and $g = 2$. For a Heisenberg spin Hamiltonian $\sum J_{nn} S_i \cdot S_j$ with the z nearest-neighbor exchange interaction J_{nn} between Ru ions, the Weiss temperature Θ is given by

$$\Theta = \frac{S(S+1)}{3} z J_{nn}, \quad (1)$$

in the mean field approximation. Using $S = 3/2$ (Ru^{5+}) and $z = 6$, we estimated the superexchange interaction $J_{nn} = -9.7$ K. Since $T_N \approx 6.5$ K and $\Theta = -73$ K, we obtain the ratio of $T_N/|\Theta| \approx 0.089$, which is nearly the same as 0.082 for VCl_2 with $S = 3/2$ (V^{4+}).²¹ These are the low dimensional characteristics of (i) and (ii). Thus, the layered compound Li_7RuO_6 is a quasi-two dimensional antiferromagnet.

In this Letter, we report ^7Li NMR studies of single crystals of triangular-lattice Heisenberg antiferromagnet Li_7RuO_6 . We found slow critical divergence with a wide critical region of $|T/T_N - 1| \leq 7$ in ^7Li nuclear spin-lattice relaxation rate, which is due to the slowing down of staggered spin fluctuations. From the analysis by renormalized classical fluctuations, we found the reduction of a spin stiffness constant, possibly due to the spin frustration effect.

Single crystals of Li_7RuO_6 were grown from the mixture of RuO_2 and a large amount of LiCO_3 flux heated in an oxygen atmosphere at 950°C . Typically $0.5 \times 0.5 \times 0.01$ mm sized and plate-like single crystals were obtained.²⁰ The plane and the vertical axes are confirmed to be the ab plane and the c axis of the quasi-hexagonal lattice, respectively. X-ray diffraction patterns for the powdered samples indicated the samples in a single phase. We performed ^7Li (nuclear spin $I = 3/2$ and nuclear gyromagnetic ratio $\gamma_n/2\pi = 16.546$ MHz/T) NMR spin-echo measurements at $H = 7.48414$ T for the samples in which the several single crystal pieces were put on a plate. The NMR frequency spectra were obtained from Fourier-transformed spin-echoes or summing them at several frequencies and frequency-swept spin-echo intensity. The ^7Li nuclear spin-lattice relaxation curves were measured by an inversion recovery technique and the relaxation

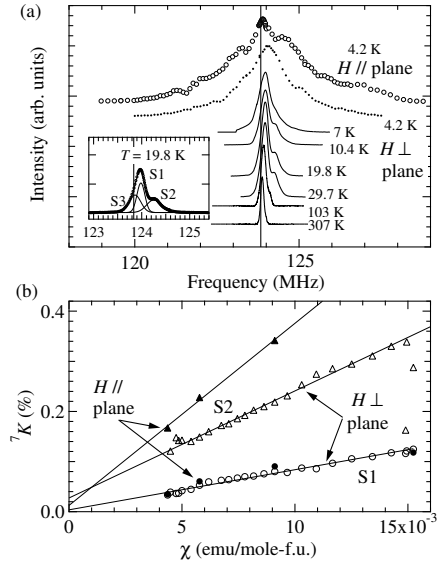


Fig. 2. (a) ^7Li NMR frequency spectra of the single crystals of Li_7RuO_6 at $H \perp$ plane (solid curves and closed circles) and at $H \parallel$ plane (open circles). The vertical line at 123.8343 MHz indicates the ^7Li NMR spectrum peak of LiClaq for a reference of zero shift. The inset shows the best fits by three Gaussian functions. (b) Knight shift 7K plotted against the bulk magnetic susceptibility χ_α with temperature as an implicit parameter.

times T_1 's were obtained from the fits by a stretched exponential function of $\exp\{- (t/T_1)^\beta\}$ (t is the time after the inversion pulse).

Figure 2(a) shows ^7Li NMR frequency spectra of the single crystals of Li_7RuO_6 at $H \perp$ plane (solid curves and closed circles) and at $H \parallel$ plane (open circles). At

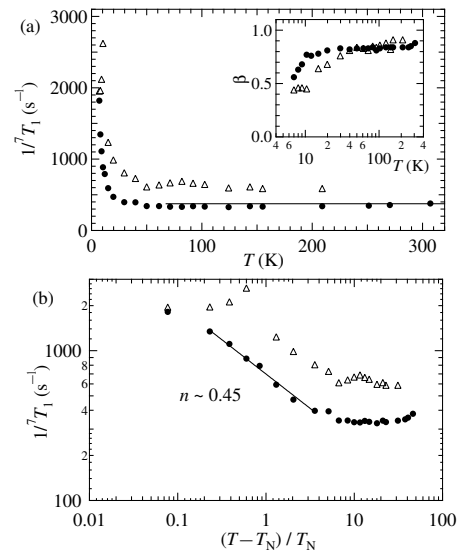


Fig. 3. (a) Temperature dependences of ^7Li nuclear spin-lattice relaxation rates $1/T_1$ of S1 (closed circles) and S2 (open triangles) at $H \perp$ plane and $T > T_N$. The inset figure shows semi-log plots of the temperature dependences of the stretched exponents β . (b) Log-log plots of ^7Li nuclear spin-lattice relaxation rates $1/T_1$ at $H \perp$ plane against the reduced temperature $(T - T_N)/T_N$.

$T > 200$ K, a single sharp ${}^7\text{Li}$ NMR spectrum and no quadrupole splits were observed. Upon cooling, the NMR spectrum shifts to higher frequency side and a weak signal separates and shifts more largely. At 4.2 K, both NMR spectra at $H \perp$ plane and $H \parallel$ plane are broadened nearly symmetrically. The featureless symmetric broadening below T_N indicates the emergence of internal magnetic field of an incommensurate staggered moments along the ab plane and the c axis.

The inset shows three Gaussian functions fit to the NMR spectrum at $H \perp$ plane and $T = 19.8$ K. A sharp strong peak and a broad higher frequency peak are denoted by S1 and S2, respectively. S3 just adjusts the foot of the spectrum, whose Knight shift is ~ 100 ppm and nearly independent of temperature. From the NMR intensity, the strong peak S1 and weak S2 can be assigned to the Li sites in the double Li layers and in the RuO_6 triangle lattice layer, respectively. The assignment at $H \parallel$ plane at $T > T_N$ not shown in Fig. 2(a) was less clear, since at least 4 peaks were observed. The lowest and highest frequency peaks are assigned to S1 and S2, respectively.

Figure 2(b) shows ${}^7\text{Li}$ Knight shifts of S1 and S2 plotted against the bulk magnetic susceptibility χ_α with temperature as an implicit parameter. The bulk magnetic susceptibility χ_α is expressed by the sum of a temperature dependent spin susceptibility χ_{spin} , the Van Vleck orbital susceptibility χ_{VV} , and the diamagnetic susceptibility of inner core electrons χ_{dia} . The ${}^7\text{Li}$ Knight shift is expressed by $K_\alpha = A_\alpha(i)\chi_{\text{spin},\alpha}/N_A\mu_B + K_{\text{dia}}$ ($i = 1$ and 2 denote S1 and S2, N_A is Avogadro's number, and μ_B is the Bohr magneton). From the $K - \chi$ plots in Fig. 2, we obtained positive hyperfine coupling constants of $A_\parallel(1) \approx A_\perp(1) = 0.45$ kOe/ μ_B , $A_\parallel(2) = 2.0$ kOe/ μ_B and $A_\perp(2) = 1.2$ kOe/ μ_B . The positive $A(1)$ and $A(2)$ indicate the predominant role of a transferred hyperfine coupling.

Figure 3(a) shows temperature dependences of ${}^7\text{Li}$ nuclear spin-lattice relaxation rates $1/T_1$ of S1 and S2 at $H \perp$ plane and $T > T_N$. The inset figure shows semi-log plots of the temperature dependences of the stretched exponents β . At high temperatures, $1/T_1$ levels off, which indicates the exchange narrowing limit. At low temperatures, $1/T_1$ shows the divergence behavior due to the critical slowing down of the staggered spin fluctuations.

In general, the high temperature limit of $1/T_1$ in the exchange narrowing is expressed by²²

$$\frac{1}{T_{1\infty}} = \sqrt{\frac{\pi}{2}} \frac{S(S+1)}{3} \frac{2\gamma_n^2 A_\parallel^2}{\omega_{\text{ex}}} \quad (2)$$

and

$$\omega_{\text{ex}}^2 = \frac{2}{3} z S(S+1) \left(\frac{k_B J_{nn}}{\hbar} \right)^2. \quad (3)$$

The hyperfine field at the in-plane Li results from the 3 nearest neighbor Ru spins. The number of the nearest neighbor exchange coupled Ru spins is 6. Putting $z = 6$, $S = 3/2$, $A_\parallel(2) = 2.0$ kOe/ μ_B and $J_{nn} = -9.7$ K for eqs. (2) and (3), we obtain $1/T_{1\infty} = 340$ s $^{-1}$, which is the same order of magnitude but slightly smaller than the actual $1/T_1 \approx 400$ and 600 s $^{-1}$ for S1 and S2 above 200

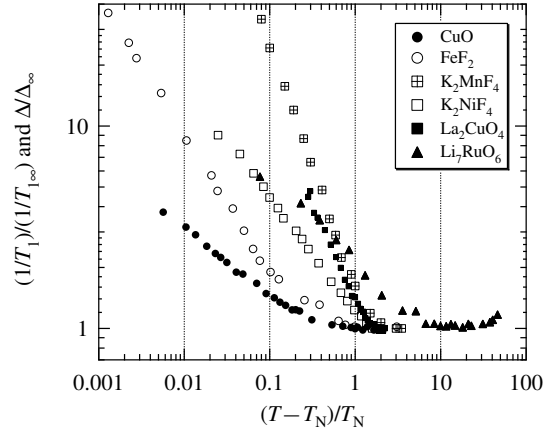


Fig. 4. Log-log plots of the nuclear spin-lattice relaxation rate $(1/T_1)/(1/T_{1\infty})$ or the continuous-wave (cw) NMR linewidth Δ/Δ_∞ against the reduced temperature $(T - T_N)/T_N$ for the critical phenomena of CuO ,²⁴ FeF_2 ,²⁵ K_2MnF_4 ,²⁶ K_2NiF_4 ,²⁷ La_2CuO_4 ,¹⁰ and Li_7RuO_6 (S1). The circles, squares and triangles are three dimensional magnets, quasi two dimensional square lattices, and a triangular lattice, respectively. The solid and open symbols are the data by spin-echo and continuous-wave (cw) measurements, respectively.

K, respectively. The experimental value of T_1 depends on the fitting function more or less. Using the fitting function of a double exponential function, we obtained a long component of $1/T_1 \approx 277$ and 435 s $^{-1}$ for S1 and S2, respectively, being the same order of magnitude of the estimated $1/T_{1\infty}$.

Figure 3(b) shows log-log plots of ${}^7(1/T_1)$ against the reduced temperature $(T - T_N)/T_N$. The critical divergence of $1/T_1$ starts from $|T/T_N - 1| \sim 7$. Although such a wide critical region is not usually regarded as a three dimensional critical region, we tried to apply a power law of $|T_N/(T - T_N)|^n$ and then obtained $n = 0.45$. This is close to the mean field value.²³

Figure 4 shows log-log plots of the nuclear spin-lattice relaxation rate $(1/T_1)/(1/T_{1\infty})$ or the continuous-wave (cw) NMR linewidth Δ/Δ_∞ against the reduced temperature $\epsilon \equiv (T - T_N)/T_N$ for the critical phenomena of CuO ,²⁴ FeF_2 ,²⁵ K_2MnF_4 ,²⁶ K_2NiF_4 ,²⁷ La_2CuO_4 ,¹⁰ and Li_7RuO_6 . The onset temperatures of the increase in $T_{1\infty}/T_1$ and linewidth Δ/Δ_∞ are the beginning of the critical slowing down of relevant spin fluctuations and indicate the width of the individual critical region. For a narrow critical region of $|\epsilon| \leq 0.1$ of CuO and FeF_2 , the critical exponent of three dimensional critical slowing down was estimated.^{24,25} The wide critical region of $|\epsilon| \leq 1.0$ of La_2CuO_4 was successfully understood by a two dimensional short range ordering effect in the renormalized classical region of the square lattice.¹⁰ The wide critical regions of square lattices K_2MnF_4 and K_2NiF_4 were also understood by the renormalized classical fluctuations.^{28,29} The critical region of $|\epsilon| \leq 7$ of Li_7RuO_6 is wider than those of the two dimensional square lattice spin systems. One should note the another striking feature of the slow divergence of $1/T_1$ of Li_7RuO_6 . The wide but slow critical divergence of $1/T_1$ characterizes

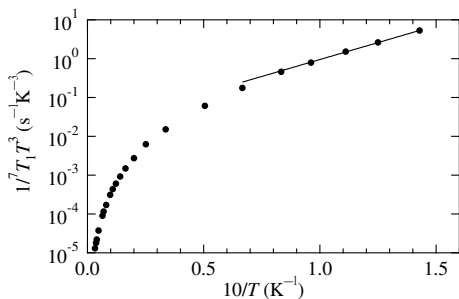


Fig. 5. Semi-logarithmic $1/T_1 T^3$ against $10/T$ for Li_7RuO_6 (S1) at $H \perp$ plane. The straight line is the fitting function of eq. (5).

the critical phenomenon of Li_7RuO_6 .

For the frustrated quantum antiferromagnets, the nonlinear sigma model description tells us the magnetic correlation length^{12, 14, 15}

$$\xi \propto \frac{1}{\sqrt{T}} \exp(4\pi\rho_\alpha/T) \quad (4)$$

with a spin stiffness constant ρ_α ($\alpha = \perp$ and \parallel plane) and the nuclear spin-lattice relaxation rate^{14, 15}

$$\frac{1}{T_1} \propto T^3 \exp(4\pi\rho_\alpha/T). \quad (5)$$

The spin stiffness constant ρ_\perp is given by

$$\rho_\perp = \frac{\sqrt{3}}{2} Z_\perp S^2 |J| \approx 1.51 |J|, \quad (6)$$

where a renormalization factor Z_\perp is estimated by a spin-wave approximation and $1/S$ expansion.^{16, 17} Equations (4) and (5) are applicable to the low temperature states at $T \ll 2\pi\rho_\alpha$.^{14, 15}

The NMR linewidth can serve as a probe of the magnetic correlation length ξ in real space. The linewidth of the S2 NMR spectrum in Fig. 2(a) increased rapidly at 70 K upon cooling, which did not scale with the Knight shift K but was similar to the divergence in $1/T_1$. Thus, we may assume the temperature dependent ξ as in eq. (4).

Figure 5 shows semi-logarithmic $1/T_1 T^3$ against $10/T$ for Li_7RuO_6 at $H \perp$ plane. The straight line is the fitting result of eq. (5). From the slope of the line at lower temperatures $T < 15$ K, we estimated the exchange interaction $|J| = 2.1$ K. Since $2\pi\rho_\perp = 20$ K, the fit range is justified *a posteriori*. The interaction $|J_{nn}| = 9.7$ K from the Weiss temperature Θ reduces to $|J| = 2.1$ K at low temperatures. Since J_{nn} should not strongly depend on temperature in the range of $4.2 \text{ K} < T < 300 \text{ K}$, the alternative reduction should trace back to the renormalization factor Z_\perp and the stiffness constant ρ_\perp . Z_\perp should reduce to about 20 % from the value in the spin-wave approximation. This reduction might be the effect of the spin frustration, e.g., the topological Z_2 vortex excitations on the spin correlation, which agrees with the numerical simulations.⁷ The reduced Z_\perp and ρ_\perp are just to put the slow divergence of $1/T_1$ in another way.

The wide critical region has been observed for the other $S = 3/2$ triangular lattice systems such as VCl_2 ,³⁰ HCrO_2 ,³¹ and LiCrO_2 .^{31, 32} It is, however, less clear

whether the slow critical divergence is ubiquitous in the triangular lattices.

In conclusion, we found slow critical divergence with a wide critical region of $|T/T_N - 1| \leq 7$ in ${}^7\text{Li}$ nuclear spin-lattice relaxation rate for the triangular-lattice antiferromagnet Li_7RuO_6 . We applied renormalized classical staggered spin fluctuations to the slow divergence and then obtained the reduction of a spin stiffness constant, suggesting the spin frustration effect.

We thank D. Mouhanna for valuable discussions. This work was supported in part by a Grant-in-Aid for Science Research on Priority Area, "Invention of Anomalous Quantum Materials," from the Ministry of Education, Culture, Sports, Science and Technology of Japan (Grant No. 16076210) and in part by a Grant-in-Aid for Scientific Research from the Japan Society for the Promotion of Science (Grant No. 19350030).

- 1) P. W. Anderson: Mat. Res. Bull. **8** (1973) 153.
- 2) E. Fradkin: *Field Theories of Condensed Matter Systems* (Addison-Wesley Publishing Co. Tokyo 1991).
- 3) A. M. Tsvelik: *Quantum Field Theory in Condensed Matter Physics* (Cambridge University Press, New York 2003).
- 4) H. Kawamura and S. Miyashita: J. Phys. Soc. Jpn. **53** (1984) 9.
- 5) H. Kawamura and S. Miyashita: J. Phys. Soc. Jpn. **53** (1984) 4138.
- 6) S. Miyashita and H. Shiba: J. Phys. Soc. Jpn. **53** (1984) 1145.
- 7) M. Caffarel, P. Azaria, B. Delamotte, and D. Mouhanna: Phys. Rev. B **64** (2001) 014412.
- 8) S. Chakravarty, B. I. Halperin, and D. R. Nelson: Phys. Rev. B **39** (1989) 2344.
- 9) S. Chakravarty and R. Orbach: Phys. Rev. Lett. **64** (1990) 224.
- 10) T. Imai, C. P. Slichter, K. Yoshimura, and K. Kosuge: Phys. Rev. Lett. **70** (1993) 1002.
- 11) R. J. Birgeneau *et al.*: Phys. Rev. B **59** (1999) 13788.
- 12) P. Azaria, B. Delamotte, and D. Mouhanna: Phys. Rev. Lett. **68** (1992) 1762.
- 13) P. Azaria, Ph. Lecheminant, and D. Mouhanna: Nucl. Phys. B **455** (1995) 648.
- 14) A. V. Chubukov, S. Sachdev, and T. Senthil: Phys. Rev. Lett. **72** (1994) 2089.
- 15) A. V. Chubukov, S. Sachdev, and T. Senthil: Nucl. Phys. B **426** (1994) 601.
- 16) A. V. Chubukov, S. Sachdev, and T. Senthil: J. Phys.: Condens. Matter **6** (1994) 8891.
- 17) P. Lecheminant, B. Bernu, C. Lhuillier, and L. Pierre: Phys. Rev. B **52** (1995) 9162.
- 18) I. S. Shaplygin, M. I. Gadzhev, and V. B. Lazarev: Russ. J. Inorg. Chem. **32** (1987) 418.
- 19) C. Mühle, A. Karpov, A. Verhoeven, and M. Jansen: Z. Anorg. Allg. Chem. **631** (2005) 2321.
- 20) K. Nakajima and H. Sato: unpublished works.
- 21) K. Hirakawa, H. Ikeda, H. Kadowaki, and K. Ubukoshi: J. Phys. Soc. Jpn. **52** (1983) 2882.
- 22) T. Moriya: Prog. Theore. Phys. **16** (1956) 23, *ibid* 641.
- 23) T. Moriya: Prog. Theore. Phys. **28** (1962) 371.
- 24) Y. Itoh, T. Imai, T. Shimizu, T. Tsuda, H. Yasuoka, and Y. Ueda: J. Phys. Soc. Jpn. **59** (1990) 1143.
- 25) A. M. Gottlieb and P. Heller: Phys. Rev. B **3** (1971) 3615.
- 26) C. Bucci and G. Guidi: Phys. Rev. B **9** (1974) 3053.
- 27) E. P. Maarschall, A. C. Botterman, S. Vega, and A. R. Miedema: Physica **41** (1969) 473.
- 28) Y. Itoh and K. Yoshimura: unpublished works.
- 29) R. J. Birgeneau: Phys. Rev. B **41** (1990) 2514.
- 30) H. Kadowaki *et al.*: J. Phys. Soc. Jpn. **56** (1987) 4027.
- 31) Y. Ajiro *et al.*: J. Phys. Soc. Jpn. **57** (1988) 2268.
- 32) L. K. Alexander *et al.*: Phys. Rev. B **76** (2007) 064429.